

# Study of Odd–Even Effect of Flexible Spacer Length on the Chain Dynamics of Main-Chain Thermotropic Liquid-Crystalline Polymers Using High-Resolution Solid-State $^{13}\text{C}$ Nuclear Magnetic Resonance Spectroscopy

Motohiro Mizuno,\* Atsuki Hirai, Hidekazu Matsuzawa, Kazunaka Endo, and Masahiko Suhara

Department of Chemistry, Faculty of Science, Kanazawa University, Kanazawa 920-1192, Japan

Motoko Kenmotsu

Tsukuba Research Laboratory, Mitsubishi Paper Mills, Ltd., 46 Wadai, Tsukuba 300-4247, Japan

Chang Dae Han\*

Department of Polymer Engineering, The University of Akron, Akron, Ohio 44325-0301

Received October 23, 2001

**ABSTRACT:** The odd–even effect of flexible spacer length on the molecular dynamics of poly-[(phenylsulfonyl)-*p*-phenylenealkylenebis(4-oxybenzoate)]s (PSHQ $n$ ) having varying lengths ( $n$ ) of methylene groups of flexible spacers and bulky pendent side groups was investigated using high-resolution solid-state  $^{13}\text{C}$  nuclear magnetic resonance (NMR) spectroscopy. The temperature dependences of  $^{13}\text{C}$  NMR spectra and spin–lattice relaxation time ( $T_1$ ) were measured for PSHQ $n$  over the temperature range of 293–520 K. Line broadening of  $\alpha\text{-CH}_2$  and rigid core carbons, due to the interference between proton decoupling and local polymer chain motion about the preferred direction of alignment accompanying the fluctuation of the rigid core, was observed in the nematic phase. The local polymer chain motion in the nematic phase was found to vary over a frequency range of  $10^4$ – $10^6$  Hz. The activation energy (77–104 kJ/mol) of this motion was found to increase with decreasing number of methylene groups and exhibits odd–even fluctuations. The motions of the local polymer chains in the nematic phase were also observed via the  $^1\text{H}$  line width in two-dimensional wideline separation (WISE) NMR spectra. It was found that the  $^{13}\text{C}$  NMR  $T_1$  of flexible spacer carbon was dominated by the fast trans–gauche exchange. The frequency of the trans–gauche exchange was found to occur above  $10^8$  Hz in the nematic mesophase, since  $T_1$  increased with increasing temperature. The activation energy (6.5–9.8 kJ/mol) of the trans–gauche exchange estimated from  $T_1$  was found to increase with decreasing number of methylene groups and exhibits odd–even fluctuations. The odd–even fluctuations of the activation energy of local polymer chain motion and trans–gauche exchange are indicative of the differences in molecular packing between PSHQ $n$  having odd-numbered  $n$  and PSHQ $n$  having even-numbered  $n$ .

## 1. Introduction

During the past 3 decades, numerous research groups have investigated phase transitions, structures of mesophase, and molecular motions of thermotropic liquid-crystalline polymers (TLCPs). There are too many papers to cite them all here. One of the most interesting experimental observations reported<sup>1–7</sup> in the early 1980s is that segmented TLCPs having even numbers of methylene groups as flexible spacer have higher clearing temperatures and larger isotropization enthalpies (and also larger isotropization entropies) than segmented TLCPs having odd numbers of methylene groups. Subsequently, other investigators<sup>8–12</sup> also reported similar experimental observations. In their studies, differential scanning calorimetry (DSC) was used to investigate phase transitions and wide-angle X-ray diffraction (WAXD) to investigate the structures of mesophase. Today, this experimental observation is referred to as the “odd–even effect” of flexible spacer length in TLCP. It should be mentioned that a few research groups<sup>13,14</sup> conducted theoretical investigations on the molecular conformation of segmented TLCPs. However, those previous studies have not unveiled the physical origin(s) of the “odd–even effect” of flexible

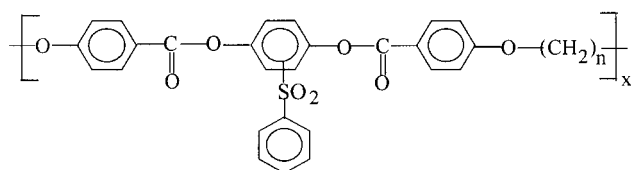
spacer length in TLCP from the point of view of local chain dynamics.

In this regard, solid-state nuclear magnetic resonance (NMR) spectroscopy is regarded as being a very powerful tool for investigating local chain dynamics associated with the “odd–even effect” of flexible spacer length in TLCP. As a matter of fact, during the past 2 decades, solid-state NMR spectroscopy has been used extensively to investigate the local structures and chain dynamics of polymeric materials. Many research groups have investigated local structures of TLCPs using solid-state NMR spectroscopy.<sup>15–40</sup> Specifically, the molecular order in TLCPs has been estimated from  $^1\text{H}$  and  $^{13}\text{C}$  NMR spectra;<sup>15–28</sup> the ratio of trans and gauche conformations in a methylene group has been determined using  $^{13}\text{C}$  NMR chemical shifts;<sup>29–31</sup> the molecular motions in TLCPs have been investigated using  $^1\text{H}$  and  $^{13}\text{C}$  NMR spin–lattice relaxation time ( $T_1$ );<sup>15,32,33,41</sup> the motion of a methylene group in TLCPs has been analyzed using models, such as rotational diffusion about a bond and rotational jump among a few sites;<sup>41</sup> the mobility at various local sites and the molecular motion in TLCPs with varying spacer lengths have been investigated using  $^{13}\text{C}$  NMR  $T_1$ ;<sup>33</sup> the  $^{13}\text{C}$  NMR spectra of the rigid

and mobile components in TLCPs have been analyzed using the difference in  $T_1$  of both components;<sup>29–31</sup> the slow director fluctuation in TLCPs has been investigated using  $^{13}\text{C}$  NMR spin–lattice relaxation time in a rotating frame ( $T_{1\rho}$ )<sup>34</sup> and the two-dimensional exchange NMR method.<sup>35,36,42,43</sup> In the high-resolution solid-state  $^{13}\text{C}$  NMR spectrum, when the frequency of the molecular motion is comparable to the proton decoupling frequency, line broadening is caused by the interference between proton decoupling and molecular motion.<sup>37–39,44</sup> Molecular motions, with frequency of the order of ca.  $10^5$  Hz, in glassy polymers have been investigated using the line width in the high-resolution solid-state  $^{13}\text{C}$  NMR spectrum.<sup>39</sup> The dynamics of each segment in the local polymer chain was investigated using two-dimensional wideline separation (WISE) NMR spectrum that produces separation of the  $^1\text{H}$  wideline spectra for different  $^{13}\text{C}$  positions.<sup>40,42,44</sup>

Despite the numerous solid-state NMR spectroscopic studies cited above, to the best of our knowledge few studies, if any, have reported on the local chain dynamics via solid-state NMR spectroscopy as it relates to the physical origin(s) of the odd–even effect of flexible spacer length in TLCP. This has motivated us to launch an investigation of local chain dynamics, via solid-state NMR spectroscopy, of well-characterized segmented TLCPs. Emphasis has been placed on the odd–even effect of flexible spacer length, because the previous DSC and WAXD studies<sup>1–12</sup> have not revealed the physical origin(s) of the odd–even effect of flexible spacer length in TLCP.

In carrying the investigation set forth, we have used poly[(phenylsulfonyl)-*p*-phenylene alkylenebis(4-oxybenzoate)]s (PSHQ $n$ ) having the chemical structure



with varying lengths ( $n = 5–12$ ) of methylene groups as flexible spacers. Earlier, Chang and Han<sup>12</sup> investigated, via DSC and WAXD, thermal transitions and the mesophase structure of PSHQ $n$  polymers. According to the study of Chang and Han,<sup>12</sup> (i) PSHQ $n$  ( $n = 4–12$ ) have a nematic phase at temperatures between their glass transition temperature ( $T_g$ ) and nematic-to-isotropic transition temperature ( $T_{\text{NI}}$ ); (ii) PSHQ3, having three methylene groups, does not exhibit liquid crystallinity; (iii) not only  $T_{\text{NI}}$  but also  $T_g$  exhibit odd–even fluctuations with varying numbers of methylene groups as flexible spacer; (iv) PSHQ $n$  having odd-numbered  $n$  exhibit a glassy nematic phase, while PSHQ $n$  having even-numbered  $n$  exhibit a crystalline nematic phase; (v) the degree of crystallinity in PSHQ $n$  having even-numbered  $n$  decreases with increasing flexible spacer length. They speculated that the experimental observations enumerated above would be closely related to the static and dynamic structures of the local polymer chains.

In this paper we present the highlights of our findings on the odd–even effect of flexible spacer length on the dynamics of the polymer chains in PSHQ $n$  using high-resolution solid-state  $^{13}\text{C}$  NMR spectroscopy. We inves-

tigated the fast motion of the flexible spacer using  $^{13}\text{C}$  NMR  $T_1$ , since  $^{13}\text{C}$  NMR  $T_1$  is sensitive to molecular motions having frequencies on the same order of NMR frequencies (ca.  $10^8$  Hz for  $^{13}\text{C}$  in the field of 7.3 T). We also investigated the slow dynamics of the local polymer chains having motions on the order of ca.  $10^5$  Hz using  $^{13}\text{C}$  NMR line width and  $^1\text{H}$  wideline spectra from WISE NMR spectra. We determined the activation energy of the molecular motions from these measurements, which enabled us to further investigate the odd–even effect of flexible spacer length on the mobility of local polymer chains. Further, we discuss the relationships between the dynamics of the local polymer chains and local structure, as affected by the flexible spacer length in PSHQ $n$ .

## 2. Experimental Section

**2.1. Materials and Sample Preparation.** In this study we used PSHQ $n$  having odd-numbered  $n$  ( $n = 5, 7, 9$ , and  $11$ ) and PSHQ $n$  having even-numbered  $n$  ( $n = 6, 8, 10$ , and  $12$ ), which were synthesized previously by Chang and Han.<sup>12</sup> Details of the synthesis procedures for PSHQ $n$  are given elsewhere.<sup>45,46</sup> The intrinsic viscosity ( $[\eta]$ ),  $T_g$ , and  $T_{\text{NI}}$  of the PSHQ $n$  polymers employed in this study are summarized in Table 1 of ref 12. For NMR measurements reported in this paper, specimens were prepared by solvent casting from dichloromethane in the presence of 0.1 wt % antioxidant (Irganox 1010, Ciba-Geigy Group) and then slowly evaporating the majority of the solvent, first at room temperature in a fume hood for 1 week and then at  $80^\circ\text{C}$  under vacuum for 3 days to remove any residual solvent.

**2.2. Solid-State  $^{13}\text{C}$  NMR Measurements.**  $^{13}\text{C}$  NMR spectrum was measured using a CMX-300 (Chemagnetics) spectrometer operating at 75.04 MHz. High-resolution solid-state  $^{13}\text{C}$  NMR spectra were obtained using magic-angle spinning (MAS) and high-power  $^1\text{H}$  dipole decoupling (DD). Cross-polarization (CP) was used for signal enhancement. The total suppression of sidebands (TOSS) sequence<sup>47</sup> was used to suppress spinning sidebands. The sample was packed into a 7.5 mm diameter zirconia rotor. The radio-frequency field strengths for CP and DD were 62.5 and 50 kHz, respectively. The contact time for the CP process was 1.0 ms, and the repetition time of accumulation was 4 s. The MAS rate was set to 4 kHz, and 4096 data points were collected over a bandwidth of 65 kHz and a dwell time of 20  $\mu\text{s}$ .

$^{13}\text{C}$  chemical shifts were expressed as values relative to tetramethylsilane (TMS) using the 29.50 ppm line of adamantane as an external reference. An average of 1000–2000 acquisition points was used to produce acceptable signal-to-noise ratios.  $^{13}\text{C}$  NMR  $T_1$  was measured by the inversion recovery method using a  $\pi-\tau-\pi/2$  pulse sequence, with repetition time greater than  $6T_1$ . The  $\pi/2$  pulse width was 4.5  $\mu\text{s}$ . MAS and DD were used for  $T_1$  measurements. Values of  $T_1$  were determined from exponential recovery of  $^{13}\text{C}$  magnetization inverted by a  $\pi$  pulse as a function of the variable delay time  $\tau$ . The peak intensity of  $^{13}\text{C}$  NMR spectrum at time  $\tau$  was measured as the  $^{13}\text{C}$  magnetization ( $M(\tau)$ ). A three-parameter equation,  $M(\tau) = M_\infty + (M_0 - M_\infty) \exp(-\tau/T_1)$ , where  $M_\infty$  and  $M_0$  are the magnetizations at  $\tau = \infty$  and 0, respectively, was used for curve fitting of the magnetization recovery. 2D-WISE spectra were measured by placing an incremental delay time ( $t_1$ ) after the  $^1\text{H}$   $\pi/2$  pulse in the standard CP-MAS experiment. For the 2D-WISE spectra, 1024 data points were acquired at a dwell time of 30  $\mu\text{s}$  with the repetition time of 4 s in the detection period ( $t_2$ ). The average of 512 acquisitions was used to produce an adequate signal-to-noise ratio. The TOSS sequence<sup>47</sup> was used to suppress spinning sidebands, and 64 data points were acquired at a dwell time of 2  $\mu\text{s}$  within time  $t_1$ , during which time the  $^1\text{H}$  wideline spectrum was recorded. Temperature calibration was done using  $^{207}\text{Pb}$  MAS spectra

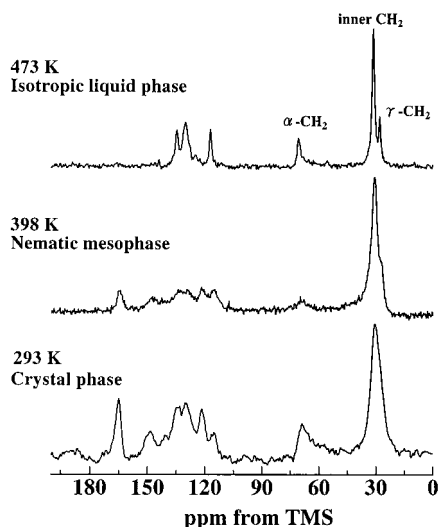


**Figure 1.**  $^{13}\text{C}$  NMR CP-MAS/TOSS spectra in each phase of PSHQ12.

of solid lead nitrate.<sup>48</sup> Signal accumulation typically started 20 min after the desired temperature was achieved.

### 3. Results and Discussion

**3.1.  $^{13}\text{C}$  NMR Spectra.** Figure 1 gives  $^{13}\text{C}$  NMR spectra for each phase of PSHQ12. Peak assignments were made using the NMR database.<sup>49,50</sup> The resonance lines at ca. 70, 30, and 26 ppm are assigned as  $\alpha\text{-CH}_2$ , inner  $\text{CH}_2$ , and  $\gamma\text{-CH}_2$  carbons, respectively, of the flexible spacer. The resonance lines of the rigid core carbons appear in the range of 105–170 ppm. The resonance line of  $\alpha\text{-CH}_2$  carbon in the nematic phase is broader than that in the other phases. Such broadening is attributable to the interference between the proton decoupling and molecular motion.<sup>37–39,44</sup> The molecular motion responsible for the width of the resonance line of the  $\alpha\text{-CH}_2$  carbon in the nematic phase is angular fluctuation of the local polymer chain about the preferred direction of alignment.<sup>34</sup> This motion is accompanied by fluctuation of the rigid core segment, since similar broadening is seen in the resonance lines of the rigid core carbons. The line widths of the  $\gamma\text{-CH}_2$  and inner  $\text{CH}_2$  carbons decrease with increasing temperature, and the apparent line broadening is not seen. The decrease in the line width of these carbons can be explained by the fluctuations of the local polymer chain that average out the distribution of the isotropic chemical shifts arising from the variety of local polymer chain conformations.<sup>39,44</sup> The fact that no appreciable line broadening of these carbons is observed indicates that the  $^{13}\text{C}\text{--}^1\text{H}$  dipole interactions of these carbons have already been averaged out to a small value by the fast exchange between the trans and gauche conformations.

**3.2. Spectral Line Width of Flexible Spacer Carbons.** Figure 2 shows the temperature dependence of the full line width at half-height ( $\delta$ ) of the  $^{13}\text{C}$  NMR spectrum for the  $\alpha\text{-CH}_2$  carbon in PSHQ7 and PSHQ12. Similar results, not presented here, were obtained for six other PSHQ $n$  polymers investigated in this study. In Figure 2 we make the following observations: (i) at temperatures below  $T_g$ ,  $\delta$  decreases gradually with increasing temperature; (ii) in the nematic region,  $\delta$  increases with increasing temperature, going through a maximum and then decreases again on the high-temperature side in the nematic phase; and (iii) in the isotropic region,  $\delta$  becomes very weakly dependent upon

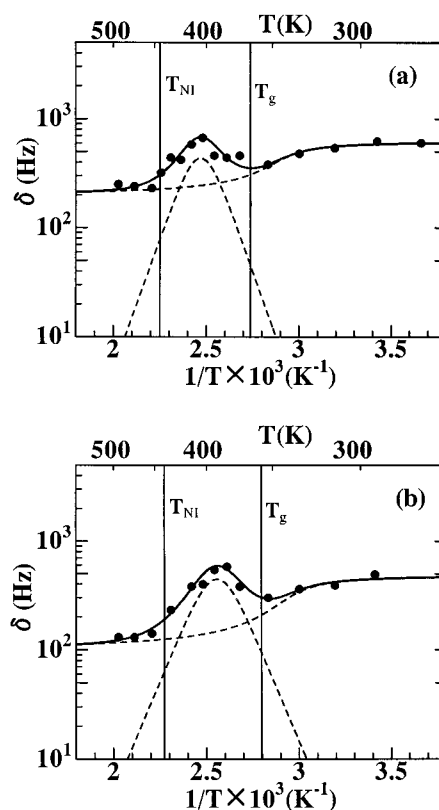


**Figure 2.** Temperature dependence of the full line width at half-height ( $\delta$ ) of  $^{13}\text{C}$  NMR spectrum for the  $\alpha\text{-CH}_2$  carbon in (a) PSHQ7 and (b) PSHQ12. The solid line shows the best fitting to eqs 1 and 2. The broken lines show each contribution.

or almost independent of temperature. The temperature dependence of  $\delta$  can be written as<sup>37–39,44</sup>

$$\delta = \delta_1 [1 + (2/\pi) \tan^{-1}(\alpha(T_0 - T))] + \Delta M_2 \tau / (1 + \omega_1^2 \tau^2) + \delta_0 \quad (1)$$

The first term of eq 1 describes the motional narrowing of line width, where  $\delta_1$  is half of the line width due to a distribution of the isotropic chemical shifts arising from a variety of local conformations of the polymer in the glassy state. The numerical constant  $\alpha$  describes the sensitivity of line width to temperature variation, and  $T_0$  is a characteristic temperature at which the first term of eq 1 becomes  $\delta_1$ . The second term of eq 1 describes the interference between the proton dipolar decoupling and the angular fluctuation of the local polymer chain about the preferred direction of alignment. Here,  $\Delta M_2$  and  $\omega_1$  represent the amount of the  $^{13}\text{C}\text{--}^1\text{H}$  second moment reduction and the strength of the decoupling, respectively. Also,  $\tau$  is the correlation time of fluctuation of the local polymer chain, and it follows an Arrhenius relation

$$\tau = \tau_0 \exp(E_a/RT) \quad (2)$$

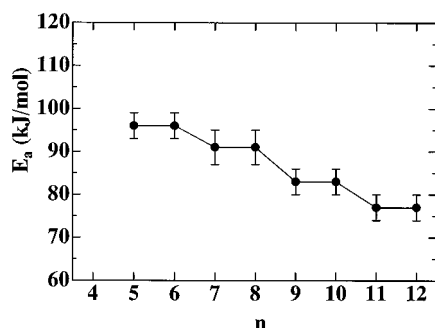
where  $\tau_0$  is the correlation time at the limit of infinite temperature,  $E_a$  is the activation energy of the motion of the local polymer chain,  $R$  is the universal gas constant, and  $T$  is the absolute temperature. The third term  $\delta_0$  of eq 1 is the line width due to the remaining distribution of local conformations at high temperatures.

Numerical values for  $\delta_0$ ,  $\delta_1$ ,  $\alpha$ ,  $T_0$ ,  $\Delta M_2$ ,  $\tau_0$ , and  $E_a$  were determined using least-squares curve fitting to eqs 1 and 2, and they are summarized in Table 1. The solid



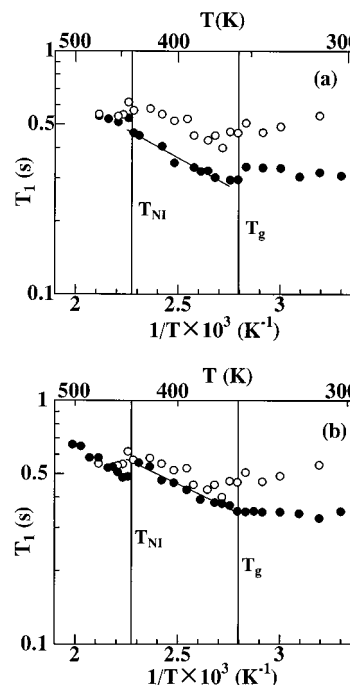
**Table 1. Parameters Obtained by Curve Fitting to the Temperature Variation of  $^{13}\text{C}$  NMR Line Width of  $\alpha\text{-CH}_2$  Carbon**

$n$	$\delta_0$ (Hz)	$\delta_1$ (Hz)	$\alpha$	$T_0$ (K)	$\Delta M_2$ (Hz $^2$ )	$\tau_0$ (s)	$E_a$ (kJ/mol)
12	100 $\pm$ 10	200 $\pm$ 10	0.05 $\pm$ 0.02	340 $\pm$ 10	(2.8 $\pm$ 0.3) $\times 10^8$	1.5 $\times 10^{-16}$	77 $\pm$ 3
11	200 $\pm$ 10	100 $\pm$ 15	0.09 $\pm$ 0.04	340 $\pm$ 10	(2.0 $\pm$ 0.3) $\times 10^8$	1.5 $\times 10^{-16}$	77 $\pm$ 3
10	120 $\pm$ 10	160 $\pm$ 10	0.04 $\pm$ 0.02	340 $\pm$ 10	(3.3 $\pm$ 0.3) $\times 10^8$	5.0 $\times 10^{-17}$	83 $\pm$ 3
9	200 $\pm$ 10	150 $\pm$ 15	0.05 $\pm$ 0.02	340 $\pm$ 10	(2.8 $\pm$ 0.3) $\times 10^8$	2.6 $\times 10^{-17}$	83 $\pm$ 3
8	100 $\pm$ 10	120 $\pm$ 10	0.13 $\pm$ 0.03	370 $\pm$ 10	(1.7 $\pm$ 0.3) $\times 10^8$	4.6 $\times 10^{-18}$	91 $\pm$ 4
7	200 $\pm$ 10	220 $\pm$ 10	0.05 $\pm$ 0.02	340 $\pm$ 10	(2.9 $\pm$ 0.3) $\times 10^8$	5.0 $\times 10^{-18}$	91 $\pm$ 4
6	120 $\pm$ 15	200 $\pm$ 15	0.03 $\pm$ 0.02	390 $\pm$ 10	(3.0 $\pm$ 0.3) $\times 10^8$	1.6 $\times 10^{-17}$	96 $\pm$ 3
5	210 $\pm$ 10	120 $\pm$ 10	0.06 $\pm$ 0.03	350 $\pm$ 10	(2.8 $\pm$ 0.3) $\times 10^8$	1.8 $\times 10^{-18}$	96 $\pm$ 3

**Figure 3.** Plots of activation energy of the local polymer chain motion ( $E_a$ ) obtained by the line width of  $^{13}\text{C}$  NMR spectrum for the  $\alpha\text{-CH}_2$  carbon vs the number of methylene groups of flexible spacer in PSHQ $n$ .

and broken lines in Figure 2 represent best-fit curves. It is seen in Table 1 that the values of  $\delta_0$  for PSHQ $n$  having odd-numbered  $n$  are larger than those for PSHQ $n$  having even-numbered  $n$ . This result, signifying that the distribution of local conformations in PSHQ $n$  having odd-numbered  $n$  is greater than that in PSHQ $n$  having even-numbered  $n$ , suggests that at high temperatures PSHQ $n$  having odd-numbered  $n$  are amorphous polymers, whereas PSHQ $n$  having even-numbered  $n$  are crystalline polymers. This supports the results reported in a previous study by Chang and Han,<sup>12</sup> who employed DSC and WAXD in their research. The frequency of the local motion of polymer chains in the nematic phase varies from  $10^4$  to  $10^6$  Hz. Figure 3 describes the dependence of  $E_a$  on the number of methylene groups in the PSHQ $n$  investigated. From Figure 3 we surmise that the flexibility of the local chains decreases with decreasing flexible spacer length, since  $E_a$  increases with decreasing flexible spacer length. In Figure 3 we observe that  $E_a$  exhibits odd–even fluctuations, indicating that PSHQ $n$  having odd-numbered  $n$  are more mobile than PSHQ $n$  having even-numbered  $n$ . Referring to Table 1 and Figure 3 summarizing the activation energies obtained from spectral line width, it should be mentioned that the variations of  $E_a$  from  $n = 6$  to 7,  $n = 8$  to 9, and  $n = 10$  to 11 are noticeable, whereas variations of  $E_a$  from  $n = 5$  to 6,  $n = 7$  to 8,  $n = 9$  to 10, and  $n = 11$  to 12 are not. At present we do not have a clear understanding of this curious observation, except to state that the values of  $E_a$  calculated have a variance (or standard deviation) of a few kJ/mol. The variance (or standard deviation) is primarily due to the nonlinear least-squares method employed to determine the value of  $E_a$  from eqs 1 and 2 having seven adjustable parameters.

According to the results published by previous investigators,<sup>13,14</sup> PSHQ $n$  polymers having odd-numbered  $n$  have out-of-plane conformation, while PSHQ $n$  polymers having even-numbered  $n$  have coplane conformation. It is then reasonable to propose that PSHQ $n$  polymers having odd-numbered  $n$  would have greater difficulty

**Figure 4.** Temperature dependence of  $^{13}\text{C}$  NMR  $T_1$  of the spacer carbons in (a) PSHQ7 and (b) PSHQ12. The filled circle (●) denotes  $T_1$  for inner  $\text{CH}_2$ , and the open circle (○) denotes  $T_1$  for  $\alpha\text{-CH}_2$  carbons.

with packing as compared to PSHQ $n$  polymers having even-numbered  $n$ . The odd–even fluctuations of activation energy observed for PSHQ $n$  polymers in the present study may help to explain the previous experimental results of Chang and Han.<sup>12</sup> They observed, via DSC and WAXD, that PSHQ $n$  polymers having odd-numbered  $n$  did not pack well, yielding glassy polymers in the solid state, whereas PSHQ $n$  polymers having even-numbered  $n$  could pack well giving rise to a well-ordered crystalline structure in the solid state.

**3.3.  $^{13}\text{C}$   $T_1$  Measurements.** Figure 4 shows the temperature dependence of  $^{13}\text{C}$   $T_1$  measurements for the flexible spacer carbons in PSHQ7 and PSHQ12. Similar results, not presented here, were obtained for six other PSHQ $n$  polymers investigated in this study. It is seen in Figure 4 that at temperatures below  $T_{\text{NI}}$  the inner  $\text{CH}_2$  carbons have a smaller  $^{13}\text{C}$   $T_1$  value than the  $\alpha\text{-CH}_2$  carbon, whereas at temperatures above  $T_{\text{NI}}$ , both carbons have almost the same  $^{13}\text{C}$   $T_1$  value. These results indicate that all  $\text{CH}_2$  carbons in the flexible spacer have the same mobility in the isotropic liquid phase, although at temperatures below  $T_{\text{NI}}$ , the inner  $\text{CH}_2$  carbons are more mobile than  $\alpha\text{-CH}_2$  carbons.  $^{13}\text{C}$   $T_1$  of inner  $\text{CH}_2$  carbons is almost independent of temperature below  $T_g$  and increases exponentially with increasing temperature above  $T_g$  (see Figure 4).

At temperatures above  $T_g$ ,  $^{13}\text{C}$   $T_1$  is dominated by fast molecular motions (above  $10^8$  Hz), since  $^{13}\text{C}$   $T_1$  increases

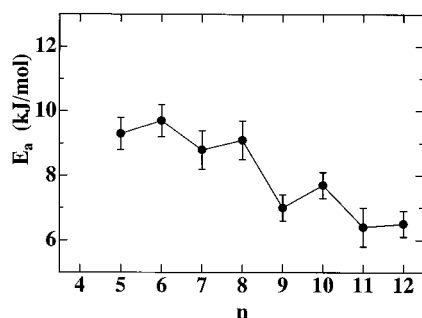


**Figure 5.** Plots of activation energy of the trans–gauche exchange ( $E_a$ ) obtained by  $^{13}\text{C}$  NMR  $T_1$  of the inner  $\text{CH}_2$  carbons vs the number of methylene groups of flexible spacer in PSHQ $n$ .

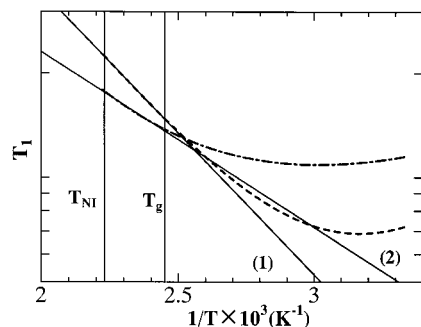


**Figure 6.** Temperature dependence of  $T_1$  of the spacer carbons: the dotted curve ( $\cdots$ ) represents the predicted values of  $T_1$  using the BPP theory, and the broken curve ( $-\cdots-$ ) represents the calculated values of  $T_1$  using the Gaussian distribution of correlation time. The straight line 1 is drawn on the linear portion of the dotted curve (BPP theory), from the slope of which the activation energy  $E_a$  is estimated to be 16 kJ/mol. The straight line 2 is drawn on the linear portion of the broken curve (based on the Gaussian distribution of correlation time), from the slope of which the activation energy  $E_a$  is estimated to be 9.6 kJ/mol.

with increasing temperature in the nematic phase. The motion correlation time of PSHQ $n$  liquid crystal system is located in the fast side of the minimum. Earlier, Silvestri et al.<sup>33</sup> reported that the activation energy  $E_a$  of the exchange between the trans and gauche conformations in the nematic phase was 12.7–17.2 kJ/mol as determined from  $^{13}\text{C}$  NMR  $T_1$  measurements. In the present study, we estimated values of  $E_a$  from the slope of the log  $T_1$  vs  $1/T$  plot in the nematic phase. Plots of  $E_a$  vs the number ( $n$ ) of methylene groups in PSHQ $n$  are given in Figure 5. The values of  $E_a$  (6–10 kJ/mol) given in Figure 5 are smaller than those reported by Silvestri et al.<sup>33</sup> This difference may be attributable to the distribution of correlation time.<sup>35,51</sup>

To elaborate on our advocacy of the distribution of correlation time, let us consider Figure 6, which shows theoretical curves for  $T_1$ . The dotted curve represents values of  $T_1$  predicted from the Bloembergen–Purcell–Pound (BPP) theory<sup>52</sup> (having a single correlation time) with  $E_a = 17$  kJ/mol, and the broken curve represents values of  $T_1$  calculated with the distribution of the correlation time. In obtaining the broken curve, the distribution of activation energy was calculated using the Gaussian distribution function with the mean value of 17 kJ/mol and the width of  $\pm 4$  kJ/mol. In the neighborhood of a minimum  $T_1$  appearing in the broken curve, the temperature dependence of  $T_1$  is very mild. If we estimate the value of  $E_a$  from the slope of the temperature dependence of  $T_1$  shown in Figure 6, we

obtain  $E_a = 9.6$  kJ/mol from the broken curve and  $E_a = 16$  kJ/mol from the dotted curve. That is, the value of  $E_a$  (9.6 kJ/mol) estimated from the consideration of the distribution of correlation time is smaller than that (16 kJ/mol) from the BPP theory.

It is of great interest to observe in Figure 5 that the activation energy of the trans–gauche exchange exhibits odd–even fluctuations, similar to that of the local polymer chain motion observed from the line width of  $\alpha\text{-CH}_2$  carbon (see Figure 3). Referring to Figure 5, the decrease in activation energy with increasing flexible spacer length indicates that the flexibility of flexible spacer increases with increasing flexible spacer length. These results are consistent with the findings of Chang and Han,<sup>12</sup> who found via WAXD that the degree of crystallinity in PSHQ $n$  having even-numbered  $n$  decreased with increasing flexible space length. The readers are reminded that PSHQ $n$  having odd-numbered  $n$  are glassy polymers.<sup>12</sup> For a series of poly(ester imide)s, however, an opposite trend was observed where the degree of crystallinity increased with increasing flexible spacer length.<sup>6</sup> It is likely that the interactions between the polymer chains contribute to retardation of the flexibility of the methylene groups in poly(ester imide)s. This effect would be enhanced by an increase in flexible spacer length in poly(ester imide)s. In the absence of the intermolecular interactions, however, the flexibility of the methylene groups is expected to decrease with decreasing number of methylene groups, since the flexibility of the methylene groups is suppressed near the rigid core. In the case of PSHQ $n$  polymers, the bulky pendent arylsulfonyl groups attached to the rigid cores will suppress the molecular packing in the polymer and the interactions between the polymer chains.

We wish to mention that in the present study we have considered two contributions—(i) the contribution between polymer chains and (ii) the contribution within a polymer chain—to the activation energy of molecular motions within the flexible spacer. As for the first contribution referred to above, our study indicates that the interaction between polymer chains increases with increasing spacer length, so that the activation energy of molecular motions within the flexible spacer increases with increasing spacer length. As for the second contribution referred to above, our study indicates that the activation energy of molecular motions within the flexible spacer decreases with increasing flexible spacer, owing to the suppression of the flexibility of the methylene groups near the rigid core. The decrease in activation energy with increasing spacer length, observed in the present study, seems to suggest that the activation energy for molecular motions within the flexible spacer is dominated by the second contribution referred to above. This observation can be understood from the point of view that the bulky pendent arylsulfonyl groups attached to the rigid cores of PSHQ $n$  polymers are expected to suppress the molecular packing in the polymer, thus making the contribution within a polymer chain predominant over the contribution between the polymer chains to the activation energy of molecular motions within the flexible spacer.

**3.4.  $^1\text{H}$  Wideline Spectra in the WISE Measurements.** WISE NMR can be used to determine the mobility of polymer chains. Figure 7 shows a stacked plot of the two-dimensional WISE-NMR spectrum for PSHQ12 at 296 K, together with the spectra sliced along

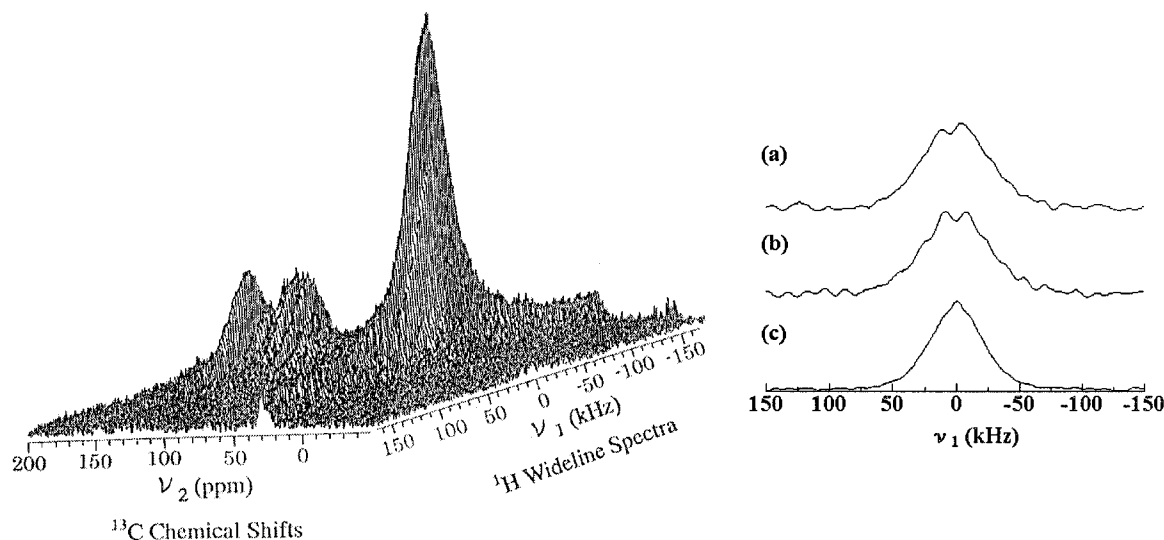


**Figure 7.** Two-dimensional WISE-NMR spectrum for PSHQ12 at 296 K, together with the spectra sliced (a) at 165 ppm (the carbon in the rigid core), (b) at 130 ppm (the carbon in the rigid core), and (c) at 30 ppm (the carbon in the flexible spacer).

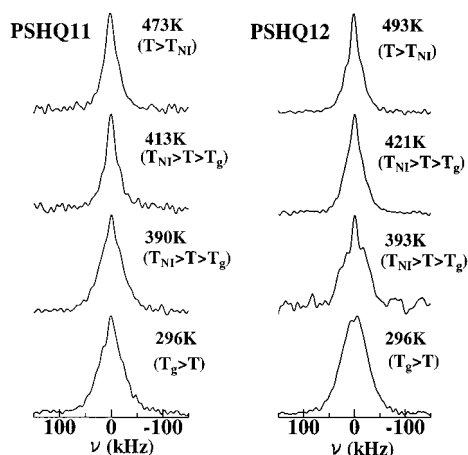


**Figure 8.** Variations of the  $^1\text{H}$  wide-line spectra of inner  $\text{CH}_2$  for PSHQ11 and PSHQ12 with temperature.

the  $\nu_1$  axis at 165, 130, and 30 ppm of  $\nu_2$  axis. For the WISE NMR spectrum, the first dimension ( $\nu_1$  axis) gives the  $^1\text{H}$  wide-line spectrum and the second dimension ( $\nu_2$  axis) the  $^{13}\text{C}$  high-resolution spectrum.<sup>40,42,44</sup> Slices along the  $\nu_1$  axis indicate the  $^1\text{H}$  wide-line spectrum for each carbon site. Figures 7a,b and 7c correspond to the  $^1\text{H}$  wide-line spectra for the rigid core segment and the inner  $\text{CH}_2$  in the flexible spacer, respectively. The full line widths at half-height of  $^1\text{H}$  wide-line spectrum for the inner  $\text{CH}_2$  and rigid core are  $55$  and  $70 \pm 5$  kHz, respectively. The narrow line width of the flexible spacer can be explained by an averaging of  $^1\text{H}$ – $^1\text{H}$  dipole interactions due to the fast exchange between the trans and gauche conformations.

Figure 8 describes the temperature variation of  $^1\text{H}$  wide-line spectra of the inner  $\text{CH}_2$  obtained by slicing along the  $\nu_1$  axis at 30 ppm of the  $\nu_2$  axis of the two-dimensional WISE-NMR spectra for PSHQ11 and PSHQ12. From the temperature dependence of  $^1\text{H}$  wide-line spectra of the inner  $\text{CH}_2$ , we observe that the mobility of PSHQ $n$  having odd-numbered  $n$  is higher than that of PSHQ $n$  having even-numbered  $n$ , because the line narrowing of the flexible spacer of PSHQ $n$  having odd-numbered  $n$  occurs at a lower temperature than that of PSHQ $n$  having even-numbered  $n$ . The  $^1\text{H}$  line width of inner  $\text{CH}_2$  decreases from ca. 55 to ca. 25

kHz on the high-temperature side in the nematic phase. Such line narrowing (the amount of the line width reduction is ca. 30 kHz) reveals the occurrence of the molecular motion of the order of  $10^5$  Hz in the nematic phase.<sup>53</sup> This motion is considered to be the same as the local polymer chain motion observed by  $^{13}\text{C}$  NMR spectral line width of the  $\alpha\text{-CH}_2$  carbon, since the frequency of this motion is in agreement with the results obtained using  $\tau_0$  and  $E_a$  in Table 1. Therefore, we conclude that the motion of local polymer chains observed in this study is accompanied by the fluctuations of the flexible spacer and rigid core segments.

#### 4. Concluding Remarks

In this paper we have shown for the first time the local chain dynamics associated with the odd–even effect of flexible spacer length in segmented TLCPs. Specifically, we have shown the existence of two kinds of molecular motion in the chains of PSHQ $n$  polymers. The slow motion of the local polymer chains in the nematic phase about the preferred direction of alignment, accompanying the fluctuations of the flexible spacer and the rigid core, was observed using the line width of  $^{13}\text{C}$  NMR spectra and  $^1\text{H}$  line width of WISE NMR spectra for PSHQ $n$  having odd-numbered  $n$  ( $n = 5, 7, 9$ , and  $11$ ) and PSHQ $n$  having even-numbered  $n$  ( $n = 6, 8, 10$ , and  $12$ ). The frequency of this local polymer chain motion in the nematic phase was found to vary from  $10^4$  to  $10^6$  Hz.

The activation energy of the local polymer chain motion increases with decreasing number of methylene groups in the flexible spacer. The increase in flexible spacer length is found to make the polymer chain more flexible and lower the clearing temperature of the nematic phase. The occurrence of fast exchange (above  $10^8$  Hz in the nematic phase) between the trans and gauche conformations in the flexible spacer of PSHQ $n$  having odd-numbered  $n$  ( $n = 5, 7, 9$ , and  $11$ ) and PSHQ $n$  having even-numbered  $n$  ( $n = 6, 8, 10$ , and  $12$ ) was confirmed by  $^{13}\text{C}$  NMR spectra,  $T_1$ , and  $^1\text{H}$  wide-line spectra of WISE NMR spectra. The activation energy of trans–gauche exchange increases with decreasing number of methylene groups in the flexible spacer. This result suggests that the interaction between polymer chains is suppressed by the bulky pendent arylsulfonyl



groups attached to the rigid backbones. Odd-even fluctuations in the activation energy, observed in this study, suggest that PSHQ $n$  having odd-numbered  $n$  are more flexible than PSHQ $n$  having even-numbered  $n$ . This explains why PSHQ $n$  having odd-numbered  $n$  cannot pack well giving rise to glassy polymers, whereas PSHQ $n$  having even-numbered  $n$  may pack well, yielding crystalline polymers.

## References and Notes

- (1) Strzelecki, L.; van Luyen, D. *Eur. Polym. J.* **1980**, *16*, 299.
- (2) Griffin, A. C.; Havens, S. J. *J. Polym. Sci., Polym. Phys. Ed.* **1981**, *19*, 951.
- (3) Antoun, S.; Lenz, R. W.; Jin, J.-I. *J. Polym. Sci., Polym. Phys. Ed.* **1981**, *19*, 1901.
- (4) Ober, C. K.; Jin, J.-I.; Lenz, R. W. *Polym. J.* **1982**, *14*, 9.
- (5) Roviello, A.; Sirigu, A. *Makromol. Chem.* **1982**, *183*, 895.
- (6) Blumstein, A.; Thomas, O. *Macromolecules* **1982**, *15*, 1264.
- (7) Krigbaum, W. R.; Watanabe, J.; Ishikawa, T. *Macromolecules* **1983**, *16*, 1271.
- (8) Jin, J.-I.; Choi, E.-J.; Ryu, S.-C.; Lenz, R. W. *Polym. J.* **1986**, *18*, 63.
- (9) Watanabe, J.; Hayashi, M. *Macromolecules* **1988**, *21*, 278.
- (10) De Abajo, J.; De la Campa, J. G.; Kricheldorf, H. R.; Schwarz, G. *Makromol. Chem.* **1990**, *191*, 537.
- (11) Pardey, R.; Shen, D.; Gabori, P. A.; Harris, F. W.; Cheng, S. Z. D.; Adduci, J.; Facinelli, J. V.; Lenz, R. W. *Macromolecules* **1993**, *26*, 3687.
- (12) Chang, S.; Han, C. D. *Macromolecules* **1997**, *30*, 1670.
- (13) Abe, A. *Macromolecules* **1984**, *17*, 2280.
- (14) Yoon, D. Y.; Bruckner, S. *Macromolecules* **1985**, *18*, 651.
- (15) Zamir, S.; Wachtel, E. J.; Zimmermann, H.; Dai, S.; Spielberg, N.; Poupko, R.; Luz, Z. *Liq. Cryst.* **1997**, *23*, 689.
- (16) Martins, A. F.; Ferreira, J. B.; Volino, F.; Blumstein, A.; Blumstein, R. B. *Macromolecules* **1983**, *16*, 297.
- (17) Mitchell, G. R.; Ishii, F. *Polym. Commun.* **1985**, *26*, 34.
- (18) Stupp, S. I.; Wu, J. L.; Moore, J. S.; Martin, P. G. *Macromolecules* **1991**, *24*, 6399.
- (19) Stupp, S. I.; Wu, J. L.; Moore, J. S.; Martin, P. G. *Macromolecules* **1991**, *24*, 6408.
- (20) Samulsky, E. T.; Gauthier, M. M.; Blumstein, R. B.; Blumstein, A. *Macromolecules* **1984**, *17*, 479.
- (21) Yoo, D. Y.; Bruckner, S.; Volksen, W.; Scott, J. C.; Griffin, A. C. *Faraday Discuss. Chem. Soc.* **1985**, *79*, 41.
- (22) Bruckner, S.; Scott, J. C.; Yoon, D. Y.; Griffin, A. C. *Macromolecules* **1985**, *18*, 2709.
- (23) Blumstein, R. B.; Blumstein, A. *Mol. Cryst. Liq. Cryst.* **1988**, *165*, 361.
- (24) Sherwood, M. H.; Sigaud, G.; Yoon, D. Y.; Wade, C. G. *Mol. Cryst. Liq. Cryst.* **1994**, *254*, 455.
- (25) Abe, A.; Kimura, N.; Tabata, S. *Macromolecules* **1991**, *24*, 6238.
- (26) Nakai, T.; Miyajima, S.; Takanishi, Y.; Yoshida, S.; Fukuda, A. *J. Phys. Chem. B* **1999**, *103*, 406.
- (27) Nakai, T.; Fujimori, H.; Kuwahara, D.; Miyajima, S. *J. Phys. Chem. B* **1999**, *103*, 417.
- (28) Silvestri, R. L.; Koenig, J. L. *Polymer* **1994**, *35*, 2528.
- (29) Cheng, J.; Jin, Y.; Wunderlich, B.; Cheng, S. Z. D.; Yandrasites, A.; Zhang, A.; Percec, V. *Macromolecules* **1992**, *25*, 5991.
- (30) Cheng, J.; Jin, Y.; Wunderlich, B.; Jonsson, H.; Hult, A.; Gedde, U. W. *J. Polym. Sci., Part B* **1994**, *32*, 721.
- (31) Ishida, H.; Kaji, H.; Horii, F. *Macromolecules* **1997**, *30*, 5799.
- (32) Silvestri, R. L.; Koenig, J. L. *Macromolecules* **1992**, *25*, 5991.
- (33) Silvestri, R. L.; Koenig, J. L.; Likavec, W. R.; Ritchey, W. M. *Polymer* **1995**, *36*, 2347.
- (34) Amundson, K. R.; Reimer, J. A.; Denn, M. M. *Macromolecules* **1991**, *24*, 3250.
- (35) Leisen, J.; Boeffel, C.; Spiess, H. W.; Yoon, D. Y.; Sherwood, M. H.; Kawasumi, M.; Percec, V. *Macromolecules* **1995**, *28*, 6937.
- (36) Spiess, H. W. *Adv. Polym. Sci.* **1985**, *66*, 23.
- (37) VanderHart, D. L.; Earl, W. L.; Garroway, A. N. *J. Magn. Reson.* **1981**, *44*, 361.
- (38) Rothwell, W. P.; Waugh, J. S. *J. Chem. Phys.* **1981**, *74*, 2721.
- (39) Takegoshi, K.; Hikichi, K. *J. Chem. Phys.* **1991**, *94*, 3200.
- (40) Schmidt-Rohr, K.; Clauss, J.; Spiess, H. W. *Macromolecules* **1992**, *25*, 3273.
- (41) Dong, R. Y. In *Nuclear Magnetic Resonance of Liquid Crystals*, 2nd ed.; Lam, L., Langevin, D., Eds.; Springer: New York, 1997.
- (42) Schmidt-Rohr, K.; Spiess, H. W. In *Multidimensional Solid-State NMR and Polymers*; Academic Press: London, 1994; Chapter 6.
- (43) Mathias, L. J., Ed.; *Solid State NMR of Polymers*; Plenum Press: New York, 1991.
- (44) Asano, A.; Takegoshi, K. In *Solid State NMR of Polymers*; Ando, I., Asakura, T., Eds.; Elsevier: Amsterdam, 1998; Chapter 10.
- (45) Furukawa, A.; Lenz, R. W. *Macromol. Chem., Macromol. Symp.* **1986**, *2*, 3.
- (46) Kim, S. S.; Han, C. D. *Polymer* **1994**, *35*, 93.
- (47) Dixon, W. T. *J. Chem. Phys.* **1982**, *77*, 1800.
- (48) Bielecki, A.; Burum, D. P. *J. Magn. Reson. A* **1995**, *116*, 215.
- (49) Rahman, A. In *Nuclear Magnetic Resonance*; Springer-Verlag: New York, 1988.
- (50) Levy, G. C.; Nelson, G. L. In *Carbon-13 Nuclear Magnetic Resonance for Organic Chemists*; Wiley: New York, 1972.
- (51) Beckmann, A. *Phys. Rep.* **1988**, *171*, 85.
- (52) Bloembergen, N.; Purcell, E. M.; Pound, R. V. *Phys. Rev.* **1948**, *73*, 679.
- (53) Abragam, A. In *The Principles of Nuclear Magnetism*; Oxford University Press: London, 1962; Chapter 10.

MA011839H